EFDA–JET–CP(12)02/41

M. Firdaouss, V. Riccardo, V. Martin, G. Arnoux, C. Reux
and JET EFDA contributors

# Modelling of Power Deposition on the JET ITER-Like Wall using the Code PFCFLUX

# Modelling of Power Deposition on the JET ITER-Like Wall using the Code PFCFLUX

M. Firdaouss[1], V. Riccardo[2], V. Martin[1], G. Arnoux[2], C. Reux[2]
and JET EFDA contributors*

***JET-EFDA, Culham Science Centre, OX14 3DB, Abingdon, UK***

*[1]CEA, IRFM, F-13108 Saint-Paul-lez-Durance, France*
*[2]EURATOM-CCFE Fusion Association, Culham Science Centre, OX14 3DB, Abingdon, OXON, UK*
** See annex of F. Romanelli et al, "Overview of JET Results",*
*(23rd IAEA Fusion Energy Conference, Daejon, Republic of Korea (2010)).*

Preprint of Paper to be submitted for publication in Proceedings of the
20th International Conference on Plasma Surface Interactions , Eurogress, Aachen, Germany
21st May 2012 - 25th May 2012

**ABSTRACT**

The development of plasma scenarios compatible with metallic wall at JET requires both reliable and accurate surface temperature measurements and power load predictions, because of the reduction of the safety margins compared to the previous carbon wall. The code PFCFlux has been developed for heat flux calculations on those components, including shadowing effects. It has been implemented at JET, for the evaluation of the power deposition on the poloidal limiters (high and low field sides) and the divertor targets. In this paper, the concepts and methodology used are described. Two cases are then analysed, one of which is compared with infrared measurements. The global efficiency of the tool is discussed, as well as the need of "end-to-end" simulation composed of several simulations tools in order to correctly predict the measurement itself.

## 1. INTRODUCTION

In JET, one of the main objective when moving from full carbon to the metallic ITER Like wall (first wall in Beryllium and divertor in Tungsten) is to assess the compatibility between high plasma performances and the choice of metal for the Plasma Facing Components (PFCs). In this context, development of plasma scenarios compatible with metallic wall requires both reliable surface temperature measurements with diagnostic and power load predictions, as the safety margins are reduced.

The operational limits have been largely taken into accounts with some uncertainty during the design phase [1]. In particular a precise investigation has been done on the first wall and divertor elements, aiming to evaluate the heat fluxes deposited during different phases [2]. The code Tokaflu [3] was used at this time, to calculate the heat fluxes as long as the shadowing on the main ILW limiters. It has proven its usability for design tasks, and confirmed globally that the design of the first wall and divertor was able to sustain the foreseen plasma scenarios.

However, the realization of one of the JET primary goals, which is to provide information on how to operate ITER with a metal wall, requires reliable diagnosis and models in order to both safeguard the ILW and permit the quantification of the heat fluxes and surface temperatures. In this framework, the development and implementation of a tool that would allow the evaluation of the expected power deposition on PFCs has been proposed. It has to be efficient enough to compute the deposited heat flux on the whole first wall and divertor at once, with a mesh necessarily fine to allow seeing the effect of small decay length, fast enough to be run on an inter-shot basis and with a friendly-user interface allowing the use by all session leaders.

From the past experience on Tokaflu and its own enhancements, CEA completely redeveloped a new tool named PFCFlux, with the same algorithms and physical modelling, but on a more modern platform. This allows to keep the same results, but with much shorter calculation time. In this step, the physic of the Scrape-Off Layer (SOL) stays simple, with a single exponential decay length. This code has then been installed at JET in order to answer to the need expressed above.

This paper first describes in section 2 the concepts and the methodology applied in the heat flux

and shadowing calculations. Section 3 explains the input and output needed for JET analysis. Section 4 shows the results of two simulations, and the qualitative comparisons with IR thermography when available. Finally, perspectives are given in the last section.

## 2. DEVELOPMENT AND METHODOLOGY

The goal of PFCFlux is to calculate shadowing pattern and parallel heat flux on any given object, for a given magnetic configuration. Both shadowing and heat flux calculations raise different issues. The shadowing calculation consists of following the magnetic field lines issued from the nodes of a meshed object (under the assumption that the particles follow perfectly the magnetic field lines) and calculating their intersection with the surrounding objects. The difficulty lies in the efficiency of the calculation, because the number of nodes and surrounding objects are potentially very large. In PFCFLux, the algorithm relies on a $2^{nd}$ order Runge-Kutta pattern, with h the step length defined by the user:

$$P_{n+1} = P_n + \frac{h}{2}\left(\left\|\dot{\vec{B}}(P_n)\right\| + \left\|\dot{\vec{B}}\left(P_n + \frac{h}{2}\left\|\dot{\vec{B}}(P_n)\right\|\right)\right\|\right) \quad (1)$$

This algorithm is well adapted to the standard magnetic configurations in tokamak. For example, a field line inside the Last Closed Magnetic Surface (LCMS) has been followed for three poloidal turns (148m). The deviation is only 3.2mm, or 0.0022%. The second order is sufficient, although the 4th order of the Runge-Kutta algorithm is also implemented. The deviation became 0.22mm (0.00014%) in this case.

The intersection of the trajectories with the surrounding objects, discretized with triangles, is ensured by a multi-threaded implementation of the Möller-Trumbore algorithm [4], which calculates the intersection of a segment with a triangle. This intersection test is what requires the most part of the computational time. Therefore it is enhanced with the use of an octree approach: the triangles forming the surrounding objects are joined in boxes. A preliminary test is done to select only the boxes containing the segment of a trajectory, in order to limit the number of time consuming operations.

For the parallel heat flux calculation, the main issue primarily comes from the knowledge of the power repartition in the SOL. This problem is more a physic modelling than a numerical issue. For now, the parallel power along a field line in the SOL is only described with an exponential decay from the LCMS, and given in the mid-plane with $\delta$ the distance to the LCMS:

$$\varphi_1(\psi) = \varphi_0 \, e^{-\frac{\delta}{\lambda_q}} \quad (2)$$

The main user inputs are the 3D magnetic field on a grid obtained through simulation or experiments, and a mesh of 3D objects facing the plasma issued. Both inputs can be as fine as wanted, and whereas it can be sufficient to have a rough grid for the magnetic field, the 3D mesh size order should not be higher than the decay length in order to see quick changes in the power deposition pattern.

## 3. INPUTS AND OUTPUTS

Tokaflu, the previous code, had strong limitations in terms of computational performances, often more than one hour for a small set of limiters at a time. The objective of PFCFlux is to allow usage during operations, with available calculation time of around 10 minutes, while taking into account the whole set of limiters and the divertor. To reach this objective, it has been installed at JET on a dedicated powerful server (2×6 cores at 2.8GHz, 12GB RAM).

The 3D models come from the drawing office models, and therefore are as close to the real objects as possible. However, a simplification must still be done, to eliminate the smallest details, like the castellation or small cuts (Fig.1). The principle limiters of ILW (excluded the dump plates at the top, whichwill be added later) and the divertor are represented by a set of 2 million of nodes and 4 millions of triangles, with a precision of around 10mm.

Magnetic grid is given by the magnetic equilibrium code EFIT, and the typical grid is 51 by 51. Both magnetic field and magnetic flux have to be defined.

The result of the calculation is basically a map of the heat fluxes overlapped with a shadowing map, but many other calculated results can be displayed, such as the incidence angle, the normal vectors, etc. Those results can be printed or exported as a text file to be used by other software.

## 4. JET SIMULATIONS

### *4.1 DETERMINATION OF THE DECAY LENGTH*

A first simulation is done with the Pulse No: 82323. The plasma configuration (Fig.2) is in limiter mode, with a contact point on the outer wall. $B_t$ is 2.5T at 2.96m, $I_p$ is 2.35MA and heating is coming from NBI (2.3MW).

With the mesh described above, a maximal trajectory length of 6m and a step length of 1mm, the calculation time is 452 seconds. Figure 3 shows the shadowed (blue) and wetted (yellow) areas for this configuration.

With the IR acquisition system [5], it is possible to get the temperature seen by the camera as a function of time. We will focus on the wide poloidal limiter 1D. The idea is to compare the temperature pattern with the heat flux deposition pattern. The picture at 10.4s, corresponding to the end time of the plasma heating, is extracted, and compared with the heat flux deposition pattern as calculated by PFCFlux. As decay length is not known precisely, different values of $\lambda_q$ are tried (Fig.4), while $\varphi_0$ is adjusted accordingly.

It is clear from the different pictures coming from the simulation that the decay length value is central for the incident heat flux pattern. For a 20mm value, the maximal heat flux is on the side of the tiles, which is not observed on the IR view. Obviously, as the decay length decreases, the peak heat flux is moving toward the LCMS, i.e. the central edge. The temperature pattern as observed is much closer to the heat flux simulated with a 5mm decay length, with fluxes and temperature concentrated near the tile centre. The main difference is that the temperature hot spot seems bigger than the maximal heat flux area.

However, the relation between heat flux and temperature is not direct, in particular the present temperature is a result of both the present heat flux but also of the past heat flux. This is especially true in the case of JET components which are not actively cooled, and therefore never at the thermal equilibrium. Moreover, with very inhomogeneous heat flux as those calculated here, heat fluxes that are occurring on the front face are spread inside the material, leading to a temperature repartition more homogenous than the heat flux repartition.

That is why the direct comparison between temperature and heat flux maps cannot be completely exact. Further thermal analysis with bi- or tri-dimensional approach would be required.

### *4.2 EFFECT OF THE LH PROTECTION RADIAL POSITION*

The LH launcher situated on the left of the narrow poloidal limiter (nPL, see Fig.1), is a movable antenna. It can be moved radially, and is normally more than 10mm behind the nPL, but not more than 35mm as it could lead to overheating of the nPL side. It can even stay ahead the nPL, during conditioning in particular.

The effect of the LH displacement is double: as it goes back, the wetted area goes toward the left nPL wing (rounded side closing the tile with a surface normal to the toroidal direction). On this surface, the incidence angle is very large, and if the decay length is also high, some strong heat fluxes may appear.

The goal of this study is to demonstrate that PFCFlux consistently shows the effect of the location of the LH frame on the power density distribution on the nPL. Note that whereas the LH and the nPL are looked by an IR camera, its low resolution (320×240) of the camera does not allow a precise understanding of the power deposition on the nPL side. Therefore no comparison will be done here with experimental data. The results of the simulations for different LH to nPL distances are presented on Fig.5.

It appears clearly from the pictures that the position of the LH protection is driving the shadowing on the nPL. At 0mm there is almost no flux on the left side of the nPL, whereas at 35mm, the nPL is wetted on all the left side on some tiles.

## 5. PERSPECTIVES

The calculation performance and ease of use of PFCFlux allow for multiple applications. This paper shows some of the possibility offered by PFCFlux to be used as a guide for the understanding of the heat flux repartition, both during shots preparation and analysis. The post shot comparison with measured temperature is the most motivating, as the example presented in this paper shows a qualitative agreement between the heat flux simulation and the temperature measured by IR.

To go toward more quantitative agreement, some improvements would have to be done, both theoretically (including more physics of the SOL, like the flux expansion, power balance…) and in the simulation itself. In particular, there is a need to develop a thermal simulation, to translate the heat flux into temperature. An option could be to facilitate the link with Ansys, and

use the heat flux from PFCFlux on a given object as an input for this same object in a classic finite-element simulation.

Expecting for even more accuracy could only be done by simulating the measurement also. Indeed, IR measurements are complicated in a metallic environment, which is very reflective. There is some discrepancy between what is measured as a temperature and the real surface temperature. The stacking of several simulations on different issues will allow having an "end-to-end" simulation chain from the plasma configuration to the camera measurement [6].

**AKNOWLEDGMENTS**

This work was supported by EURATOM and carried out within the framework of the European Fusion Development Agreement. The views and opinions expressed herein do not necessarily reflect those of the European Commission.

**REFERENCES**

[1]. V. Riccardo et al., Physica Scripta **138** (2009) 014033

[2]. M. Firdaouss et al., Journal of Nuclear Materials **390-391** (2009) 947

[3]. R. Mitteau et al., Journal of Nuclear Materials **313-316** (2003) 1229

[4]. T. Möller, B. Trumbore, Journal of Graphic Tools, **2** (1) (1997) 21–28

[5]. V. Martin et al., Fusion Engineering and Design, **86** (4-5), 270

[6]. M-H. Aumenier et al., to be published in Review of Scientific Instruments as part of the Proceedings of the 19th Topical Conference on High-Temperature Plasma Diagnostics (HTPD), Monterey, California, May, 2012

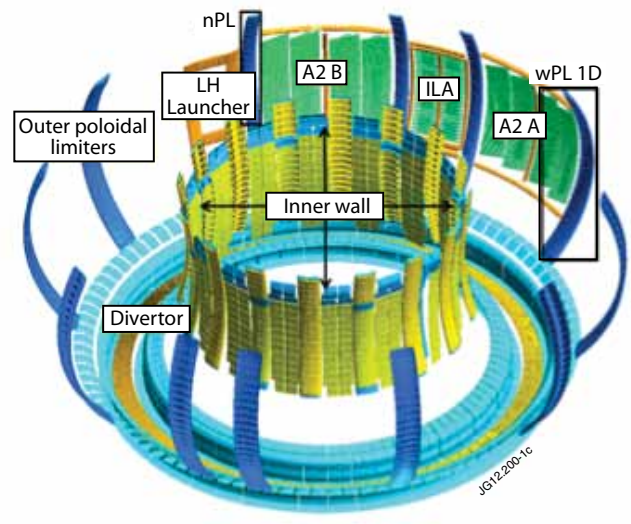


*Figure 1: JET internal components*

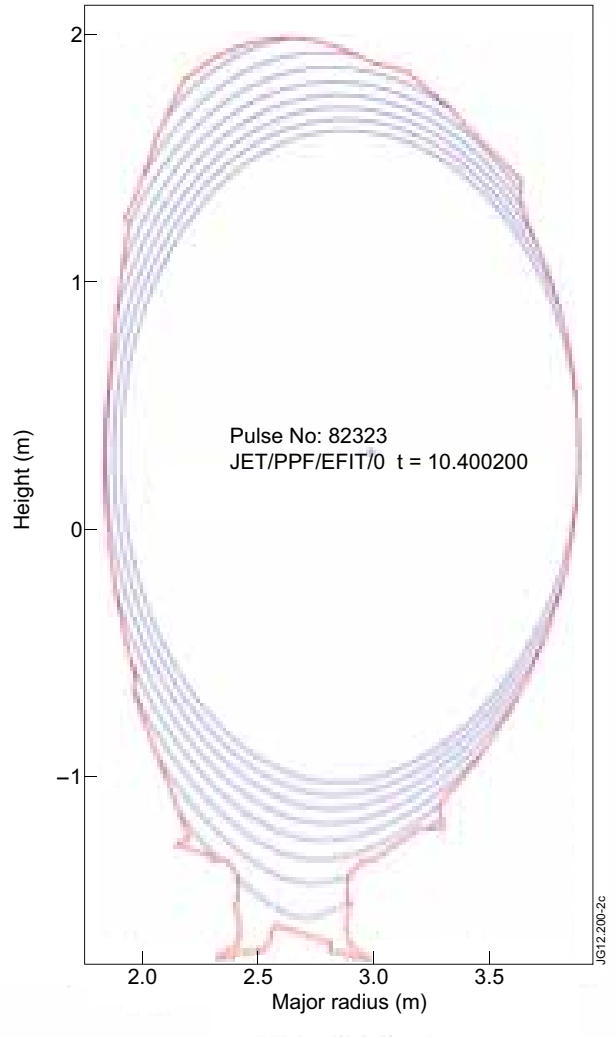


*Figure 2: Magnetic flux iso surfaces – Pulse No: 82323 at 10.4s*

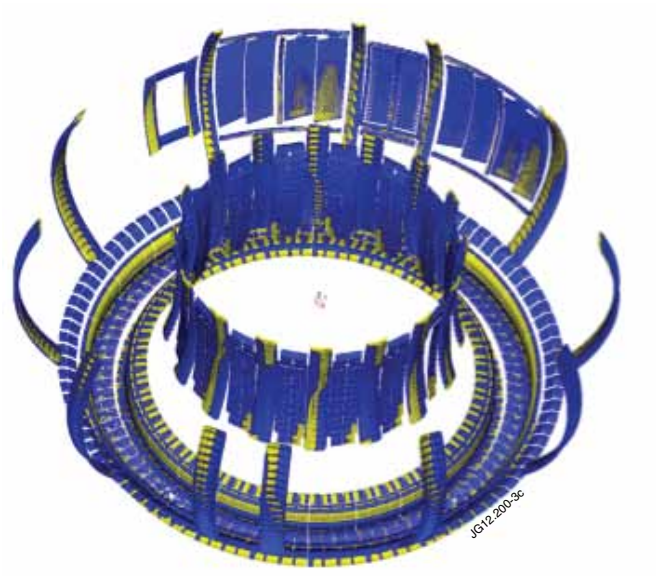


*Figure 3: Shadowing map on all the internal components (ILW + divertor).*

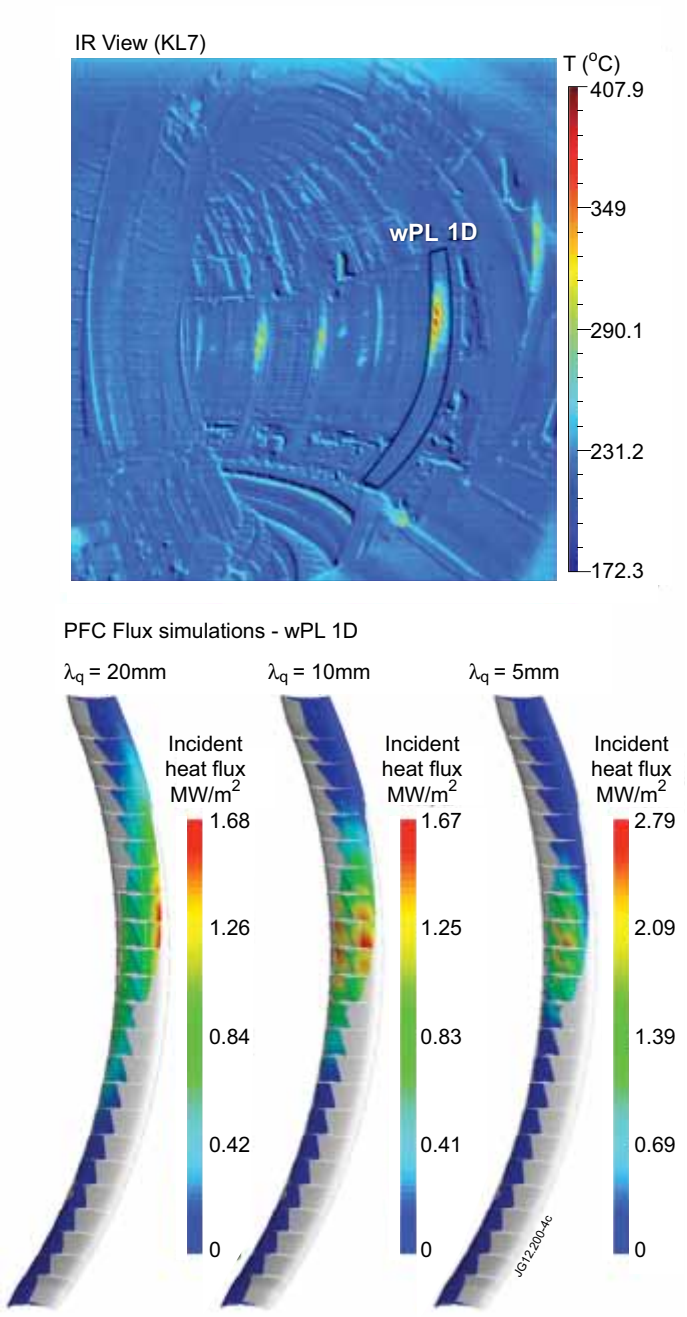


*Figure 4: Comparison of the temperature measured by the camera KL7 with the heat flux calculated with PFCFlux for different decay length (shadowed area in grey).*

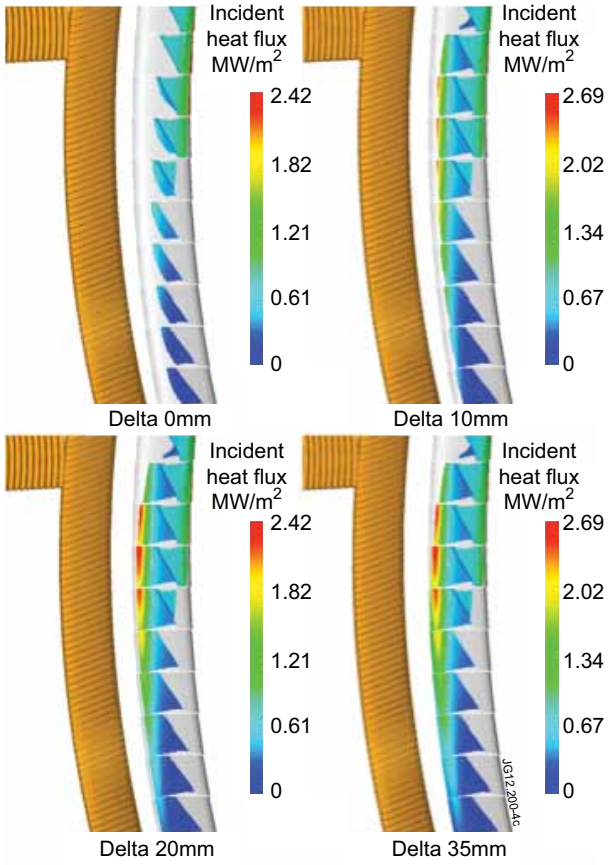


*Figure 5: Evolution of the heat flux deposition on the nPL for different LH radial positions*